

# Guiding light along an infinitesimal line between impedance surfaces

Dia'aaldin J. Bisharat<sup>\*1,2</sup> and Daniel F. Sievenpiper<sup>2</sup>

<sup>1</sup>*Department of Electronic Engineering, City University of Hong Kong, Kowloon, Hong Kong, China*

<sup>2</sup>*Electrical and Computer Engineering Department, University of California, San Diego, California, 92093, USA*

*\*dbisharat2-c@my.cityu.edu.hk; dsievenpiper@eng.ucsd.edu*

We report a new electromagnetic mode at the interface between two planar surfaces and demonstrate an open boundary structure capable of confining and guiding waves along a one-dimensional line object. The mode is determined by complementary isotropic impedance boundary conditions and is experimentally verified using patterned conductor surfaces. The line wave possesses a singular field enhancement, unidirectional propagation, wide bandwidth and tunable field confinement properties, which may advance applications of topological photonic insulators. These properties are tested at different scenarios and potential applications are proposed. Our approach opens a new door to manipulating electromagnetic waves, which is fundamental to modern sensing and communication technologies, as well as quantum information processing schemes.

Having a peak field bound to the planar interface of dissimilar media makes surface waves (SWs) [1] attractive for devising signal transmission and routing with simple implementation for sensing and communication applications [2, 3]. Exploiting surface plasmon polaritons' (SPPs) nature [4, 5], SWs can also exhibit strong light confinement which is useful for realizing subwavelength guiding structures and as a result potentially high-density integration of optical circuits and lower waveguide bending loss. However, this approach suffers from high propagation loss; hence modifications such as V-shaped grooves [6, 7] and metallic wedges [8] were proposed at the expense of added complexity. In the latter case, the wave mode is reduced to one dimension despite the absence of an enclosing structure, thus enabling greater guiding control. Similarly, guided waves in air at the edge of photonic crystals (PhCs) have been numerically studied [9]. However, these modes rely on intricate lattice configuration and creating simultaneous bulk and surface bandgaps; hence they are limited in bandwidth.

The recent advent of topological insulators [10,11] has promoted extensive research on interface states with one-way wave propagation that is immune to backscattering due to imperfections in host materials, which would bring forth robust

optical circuitry [12]. Successful demonstrations are based on breaking time-reversal or spatial-inversion symmetry using magnetic materials [13,14,15,16] or temporal modulations emulating the effect of an external magnetic field [17, 18]. Other implementations include bianisotropic metamaterials with superlattice arrangements [19,20,21], in which artificial symmetries and nontrivial topology of bulk states give rise to spin-polarized states locked to the wavevector. Also, control over topologically nontrivial states was theoretically demonstrated in chiral hyperbolic metamaterials [22] based on an effective medium approach [23,24,25] in contrast to PhCs-based states [13,14,15,16,18,19,20, 21,26,27], which require precise arrangements of finely tuned materials. Furthermore, a topologically protected mode inside a spin-filtered waveguide has been shown possible by enforcing perfect-electric-conductor (PEC) and perfect-magnetic-conductor (PMC) boundaries [28]. This approach permits wider bandwidth than earlier techniques, yet requires a non-planar configuration that hinders fabrication in high-frequency regimes, and is not suitable for device integration.

In this work, we introduce a new one-dimensional mode, analogous to SWs, that is confined to the line interface between two planes, and propagates in air without the need for any

enclosing structure. Besides forming the smallest waveguide possible, the line mode has intrinsic topological properties including unidirectional and reflection-free propagation though is free from the restrictive requirements of earlier concepts. Unlike existing topological photonic insulators (TPIs), our approach enables a broad bandwidth, is a realistic 3D system with an open boundary, and does not require any bulk media. Furthermore, the mode exhibits unique properties of singular field enhancement and tunable spatial field confinement. We establish conditions for the mode's existence by characterizing the interfaced planes merely by complementary isotropic surface impedances. Also, we provide measurement results demonstrating the feasibility of using periodic surfaces with certain effective medium properties, such as simple frequency-selective-surfaces (FSS) as a proof-of-concept. Importantly, since our design functions with subwavelength patterns, it provides a flexible and simple platform for investigating and manipulating highly confined topological states with subwavelength resolution. As such, our work paves the road for planar, compact and efficient routing and concentration of electromagnetic energy in the microwave and optical regimes and opens the door for unconventional devices.

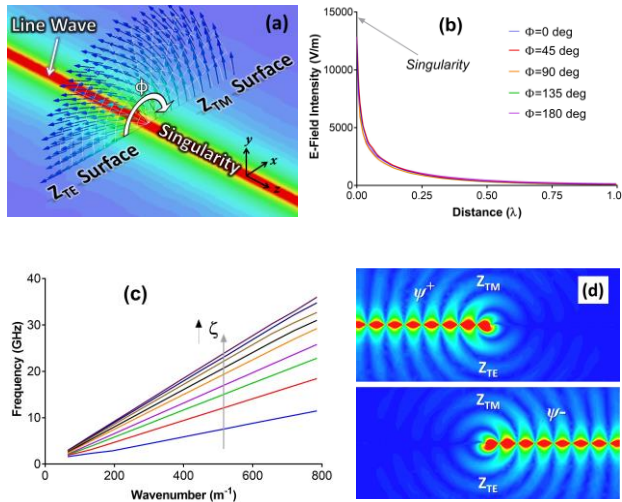


FIG. 1 (color online). Fields characteristics of the line wave mode. (a) Magnitude distribution and vector plot of the electric field above the TE and TM surfaces across the line interface showing the line wave mode (linear scale), (b) decay curves of the electric field at different directions around the line interface, (c) dispersion curves of the line mode at different values of complementary impedances across the interface, and (d) pseudo-

spin states of line wave excited by electric and magnetic Hertzian dipoles in phase (above) and out of phase (below).

SW modes can be guided on planar structures with subwavelength periodic inclusions, known as metasurfaces [29,30], whose response to impinging waves and their guiding properties can be conveniently characterized by surface impedance [31,32]. This methodology has been extensively used for variety of applications including EM guiding, absorption, radiation, scattering alteration, cloaking, and self-focusing [33,34,35,36,37,38]. Consider a field with an exponential decay  $e^{-\alpha y}$  away from the surface and a propagation function  $e^{-j\beta z}$ , such that  $\alpha^2 = \beta^2 - k^2$ , where  $k$  is the wavenumber in the free space. The surface impedances for transverse-magnetic (TM) and transverse-electric (TE) polarized waves are [39]:

$$Z_{TM} = j\eta_0 \frac{\alpha}{k} \quad (1.1)$$

$$Z_{TE} = -j\eta_0 \frac{k}{\alpha} \quad (1.2)$$

where  $\eta_0$  is the intrinsic impedance of free space. Meanwhile, the refractive index  $n$  seen by the SW is:

$$n = \frac{c}{v_p} = \frac{\beta}{k} \quad (2)$$

where  $c$  is the speed of light in free space and  $v_p$  is the phase velocity of the wave along the surface. Therefore, the relationship between the surface impedance and the refractive index is given by [40]:

$$Z_{TM} = \eta_0 \sqrt{1 - n^2} \quad (3.1)$$

$$Z_{TE} = \eta_0 / \sqrt{1 - n^2} \quad (3.2)$$

Thus, the impedances which would support TM- and TE-polarized SWs to propagate with equal phase velocities can be calculated as follows:

$$j \frac{Z_{TE}}{\eta_0} = j \frac{\eta_0}{Z_{TM}} = \zeta \quad (4.1)$$

$$Z_{TM} = j\eta_0 / \zeta \quad (4.2)$$

$$Z_{TE} = -j\eta_0 \times \zeta \quad (4.3)$$

where  $\zeta$  is a real number. First, consider the case where  $\zeta$  is infinite, so that the TM-surface becomes a PEC while the TE-surface becomes a PMC. Obviously, the PEC (PMC) surface forces the tangential electric (magnetic) field to vanish, thus allowing only the TM (TE) SW mode to survive. When interfacing PEC and PMC surfaces, a new mode that is localized at the interface appears. The new mode is a product of interference between TM and TE modes, which are only supported at either side of the interface. As a result, given the open boundary nature of the resultant structure, the mode decays away from the interface line. As the cross-sectional view in Fig. 1a shows, the electric field vectors point in the transverse direction adjacent to the  $Z_{TE}$  surface and vary gradually toward the normal direction as we trace a path of constant distance away from the interface line towards the  $Z_{TM}$  surface. Hence, it is straightforward to represent this waveguide configuration in cylindrical coordinates and the waveform of the mode is deduced as [41]:

$$E_z = E_0 K_{\frac{1}{2}}(\alpha \rho) \text{Sin}\left(\frac{\phi}{2}\right) e^{-j\beta z} \quad (5.1)$$

$$H_z = \frac{E_0}{\eta_0} K_{\frac{1}{2}}(\alpha \rho) \text{Cos}\left(\frac{\phi}{2}\right) e^{-j\beta z} \quad (5.2)$$

where  $K$  is the modified Bessel function of the second kind, and  $\alpha^2 = k^2 - \beta^2$ , with  $\beta \geq k$ .

The waveform is verified with full wave simulation in ANSYS HFSS software, which clearly shows the singular nature of field intensity at the interface line as depicted in Fig. 1b. Here, for a given  $\zeta$  value, the field intensity decays away from the interface at different  $\phi$  angles at the same rate. Note that although the field is infinite at the line, the field everywhere has a finite integral and thus the power carried by the line wave is finite. Just as SWs on perfect conductors are only loosely bound to the surface, this is also the case for line waves, which have  $\beta = k$  for the limit of a PEC-PMC interface. A more tightly bound mode is readily attainable by adopting a finite  $\zeta$  value, hence  $\beta > k$ , as shown in Fig. 1c, with smaller  $\zeta$  resulting in slower mode. Note that regardless of the  $\zeta$  value, the field remains infinite at the line in the absence of loss.

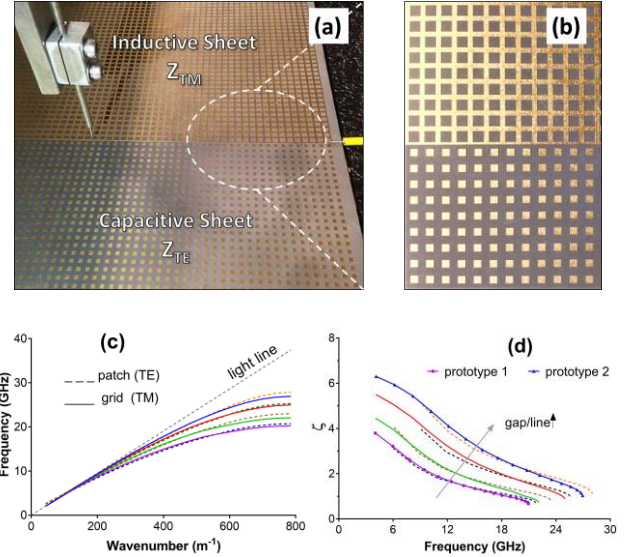


FIG. 2 (color online). Measurement setup and characteristics of the fabricated FSS sheets. (a) A probe antenna (right) oriented along the interface line is used as the excitation source while another probe (left) oriented vertically at a 2mm distance above to the surface is used to scan the relative intensity of the normal component of electric-field, (b) zoom in of the complementary FSS sheets fabricated on a printed-circuit-board (PCB) on Rogers RT/duroid 5880 ( $\epsilon_r = 2.2$ ) substrate with a 0.8mm thickness, (c) dispersion characteristics of TM and TE FSS cells of different sizes, and (d)  $\zeta$  values versus frequency for different sizes of FSS cells. Prototypes 1 and 2 both have unit cell period of 4mm. Prototype 1 (2) has grid line width of 0.2mm (1.2mm) and gap width of 0.8mm (2.2mm) between patches. The difference between the sizes of the complementary FSS cells is to compensate for the substrate permittivity.

To realize the line wave, two surfaces whose impedances take the form in equation (4) are required, that is an inductive surface to support a TM mode and a capacitive surface to support a TE mode. These criteria can be fulfilled by simple frequency-selective surfaces (FSS) such as these shown in Fig. 2b. Here, the conducting patches (strips) exhibit a dominant capacitive (inductive) response at frequencies where the FSS cell is subwavelength. Fig. 2c shows that the respective SW modes of the complementary surface have dispersion curves that overlap over a wide frequency band. Therefore, TM- and TE-mode of the same phase velocity [42] are supported and a line wave could be supported at their interface. Two prototypes with interfaced FSS sheets were prepared, whose constitutive unit cells' size corresponds to about  $\lambda_0/12$  at 6GHz and to about  $\lambda_0/4$  at 18GHz, where  $\lambda_0$  is the wavelength in free space. Fig. 2d shows the associated  $\zeta$  values at

different frequencies, which are higher in the case of prototype 2.

Fig. 3a, which maps the relative intensity of the normal component of electric field above the impedance surfaces, clearly demonstrates higher field concentration at the line interface compared to that on either side. The measured results also show successful excitation and transmission of the line wave for a distance of several wavelengths at different frequencies. Notably, Fig. 3b exhibits a spatial confinement of energy with a small fraction of the wavelength across the interface line. The electric field component normal to the surface is evident on both sides of the interface, albeit with slightly larger amplitude on the TM side (the positive x-axis of Fig. 3b), which verifies that the line mode has necessarily a composite of TM and TE properties. Moreover, due to lower  $\zeta$  values, prototype 1 exhibit greater field concentration than prototype 2, as expected. The measured operation range, which spans about two octaves of bandwidth, could be extended by adopting other complementary artificial surfaces with lower dispersion and whose dispersion curves overlap over a larger frequency range. Likewise, the fields at the singularity are limited in physical implementations by the thickness of the surface, the substrate loss tangent, and the periodicity of the FSS structures.

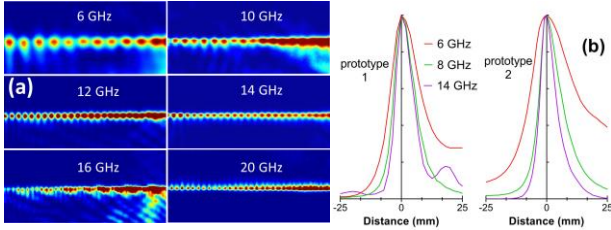


FIG. 3 (color online). Measured results of the line wave. (a) Electric field magnitude distribution at different frequencies on top of prototype 1 (left) and prototype 2 (right), and (b) normalized decay curves of the normal component of electric field away from the interface (linear scale) above the two prototypes.

Another important aspect is that the line wave exhibits topological properties—reflection-free wave transport and one-way propagation. In a medium like air, duality is preserved, naturally giving rise to two decoupled pseudo-spin states. PEC and PMC boundaries violate the duality since they have opposite effects on the electric and magnetic

components of the fields. However, joined PEC and PMC boundary conditions may preserve duality symmetry, for instance having PEC ( $\epsilon = -\infty$ ,  $\mu = 1$ ) and PMC ( $\epsilon = 1$ ,  $\mu = -\infty$ ) walls form a pair of mirror images, and hence satisfy the  $\epsilon(z) = \mu(-z)$  symmetry [28]. Such alternating parallel plate configuration is not compulsory though, as a single PEC-PMC interface is sufficient due to  $\epsilon$ -negative or  $\mu$ -negative materials possessing different topological orders [43, 44]. Obviously, both materials support evanescent waves but possess opposite signs of imaginary impedance. As a result, new modes emerge that are a combination of magnetic and electric modes with a specific phase relationship, hence conserved pseudo-spin values. Furthermore, since the pseudo-spin configuration is uniquely defined by the direction of the mode wavevector ( $k$ ), the interface constitutes a spin-filtered channel.

The approach above can be generalized to include the formation of domain walls by the inversion of surface impedance; that is interfacing inductive/capacitive surfaces with identical  $\zeta$  value. Note that besides offering design flexibility and additional control over the properties of the interface states, this generalization solves the issue of the weak cross coupling between TM and TE modes in the PEC-PMC case, which otherwise necessities using a closed waveguide configuration for practical applications. The paradigm of effective surface impedance has been exploited in relation with band geometric (Zak) phases to explain the appearance of interface states in 1D and 2D systems of PhCs [45, 46, 47]. Although approaches such as using mutually inverted 2D dielectric PhCs have also been studied, there is no mechanism in this principle that dictates the transport properties of the interface state [48]. In comparison, our structure is free of the bandwidth limitation associated with PhCs and constitutes a spin-filtered channel as evident in Fig. 1d. Similar to the spin-polarizations exhibited in TPIs, the proposed line wave mode has counter propagating pseudo spin-states up ( $\psi^+$ ) and down ( $\psi^-$ ) for electric and magnetic field components that are in phase and out of phase, respectively.

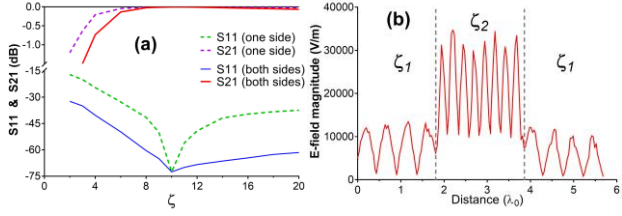


FIG. 4 (color online). Influence of a finite discontinuity in surface impedance on the line wave. (a) Transmission and reflection coefficients of the mode due to the defect at one or both sides of the interface over a distance of  $0.6\lambda_0$ , and (b) snapshot of field magnitude depicting an increased enhancement and a shorter wavelength over a finite distance due to change in surface impedances across the line interface.

The one-way propagation feature endows our line guide with protection against reflection due to structural defects. To verify this topological property, we introduce a discrete discontinuity in surface impedance along the interface line. As shown in Fig. 4a, for a large range of varied  $\zeta$  values over a distance of  $0.6\lambda_0$  in either one or both impedance surfaces, reflection coefficient ( $S_{11}$ ) lower than -30dB and isolation ( $S_{21}$ ) of about -0.1dB is achieved. This is expected given that such defect does not violate spin-degeneracy or cause reversal of boundary conditions. By taking advantage of this robustness, we could intentionally alter the surface impedances, i.e.  $\zeta$  value, simultaneously across the interface to control the spatial field confinement of the line mode and its propagation constant as shown in Fig. 4b. For example, this enables the design of compact delay lines and phase shifters without the need for any bends and without occupying any additional space. On the other hand, switching the sign of the surface impedance across the interface would cause total reflection of the interface mode. This feature is useful for building non-reciprocal devices such as isolators and circulators with simple implementation in microwave and photonic applications, unlike most existing structures. For example, Fig. 5a shows that the junction due to the surface impedance reversal forms a four-port network that functions as a common microwave magic-T structure, where the line wave fed at port 1 is guided to ports 2 and 4 with no energy coupling to port 3 as desired.

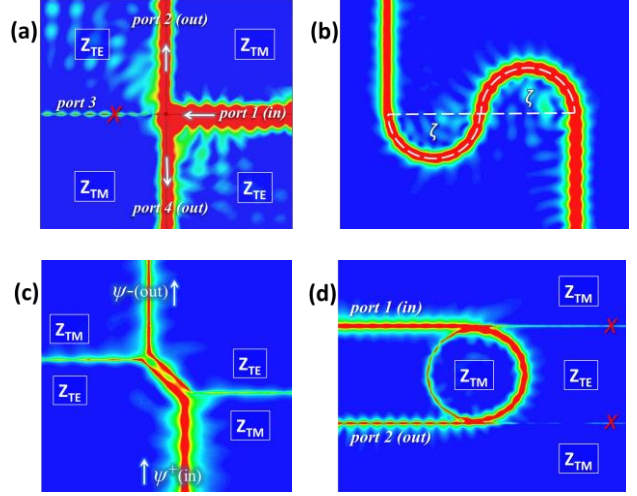


FIG. 5 (color online). Potential application of the line wave. (a) Wave transmission in four-port network (magic-T) of a junction due to surface impedance reversal, (b) wave transport along a curved interface line with a proper change in TM and TE surface impedances restoring equal phase velocity at the two sides, (c) coupler structure showing excitation of a reversed pseudo-spin mode, and (d) an implementation of a ring-resonator showing frequency selection.

One the other hand, guiding the line mode along a bent path seems to cause scattering. This is due to the curvature causing the phase velocities of the wave on both sides of the interface to differ, thus resulting in a leakage similar to that of conventional SW mode along a curved surface. This is different from existing TPIs, which have a complete bandgap in the bulk where no modes can exist. Although the eigenfields of the proposed line mode must be localized near the interface, energy can couple to the SW modes that are supported at the same frequency on the surrounding surfaces. Nevertheless, we can prevent such leakage by compensating for phase velocity difference through adjusting the relative impedance values; hence restoring the original relative boundary conditions, as depicted in Fig. 5b. Here, a relatively lower  $\zeta$  value was used in the dotted semi-circular area inward the curve in order to increase the propagation constant, i.e. shorten the wavelength, of the SW mode propagating in that region so that the two phase fronts across the interface would move along the line at the same speed. This ability to couple to SW modes can be useful for unique applications. For example, Fig. 5c shows a coupler design that enables transferring energy between two eigenfields of opposite spin-polarizations in nearby waveguides. In addition, the

line wave can be used in a ring resonator design as illustrated in Fig. 5d for filtering applications.

The above findings make the line wave appealing for energy confinement and transport applications, as a one-dimensional object being potentially the smallest waveguide possible. In addition, due to its spin-polarization property and planar configuration, the line wave may be used to integrate with 2D electronic topological insulators [49]. It also has a strong mode confinement which is a prerequisite for enhanced light-matter interactions [50]. Moreover, the field singularity of the mode as well as having an air channel at the line interface can be potentially used to free electrons from materials and guide them in air free of scattering, offering by that a simple implementation of high speed micro-plasma and vacuum based electronic devices [51]. Furthermore, our approach based on surface impedance boundary conditions allows for topological photonic insulators with reconfigurable pathways [52], for instance, through electrostatic biasing in graphene [53]. This tuning capability in addition to the field singularity can also pave the way to nonlinear photonic structures for switching and modulation applications [54].

This work has been supported in part by AFOSR grant FA9550-16-1-0093.

---

[1] J. A. Jr. Polo, T. G. Mackay, and A. Lakhtakia, *Electromagnetic Surface Waves: A Modern Perspective*, 1st ed. (Elsevier Inc., London, 2013)

[2] J. Homola, *Surface Plasmon Resonance Based Sensors* (Springer, 2006)

[3] M. Dragoman and D. Dragoman, *Prog. Quantum Electron.* **32**, 1–41 (2008)

[4] W. L. Barnes, A. Dereux, and T. W. Ebbesen, *Nature* **424**, 824–830 (2003)

[5] A. V. Zayats, I. I. Smolyaninov, and A. A. Maradudin, *Phys. Rep.* **408**, 131–314 (2005)

[6] I. V. Novikov and A. A. Maradudin, *Phys. Rev. B* **66**, 035403 (2002)

[7] S. I. Bozhevolnyi, V. S. Volkov, E. Devaux, J. Y. Laluet, and T. W. Ebbesen, *Nature* **440**, 508–511 (2006)

[8] E. Moreno, S. G. Rodrigo, S. I. Bozhevolnyi, L. Martín-Moreno, and F. J. García-Vidal, *Phys. Rev. Lett.* **100**, 023901 (2008)

[9] L. Lu, J. D. Joannopoulos, and M. Soljačić, *Phys. Rev. Lett.* **108**, 243901 (2012)

[10] M. Z. Hasan and C. L. Kane, *Rev. Mod. Phys.* **82**, 3045–3067 (2010)

[11] X. L. Qi and S. C. Zhang, *Rev. Mod. Phys.* **83**, 1057–1110 (2011)

[12] L. Lu, J. D. Joannopoulos, and M. Soljačić, *Nature Photon.* **8**, 821–829 (2014)

[13] Z. Wang, Y. Chong, J. D. Joannopoulos, and M. Soljačić, *Nature* **461**, 772–775 (2009)

[14] F. D. M. Haldane and S. Raghu, *Phys. Rev. Lett.* **100**, 013904 (2008)

[15] Z. Wang, Y. D. Chong, J. D. Joannopoulos, and M. Soljačić, *Phys. Rev. Lett.* **100**, 013905 (2008)

[16] Y. Poo, R. X. Wu, Z. Lin, Y. Yang, and C. T. Chan, *Phys. Rev. Lett.* **106**, 093903 (2011)

[17] K. Fang, Z. Yu, and S. Fan, *Nature Photonics* **6**, (2012) 6, 782–787 (2012)

[18] M. C. Rechtsman et al., *Nature* **496**, 196–200 (2013)

[19] A. B. Khanikaev et al., *Nature Mater.* **12**, 233–239 (2013)

[20] T. Ma, A. B. Khanikaev, S. H. Mousavi, and G. Shvets, *Phys. Rev. Lett.* **114**, 127401 (2015)

[21] A. P. Slobobzanyuk, A. B. Khanikaev, D. S. Filonov, D. A. Smirnova, A. E. Miroshnichenko, and Y. S. Kivshar, *Sci. Rep.* **6**, 22270 (2016)

[22] W. Gao et al., *Phys. Rev. Lett.* **114**, 037402 (2015)

[23] N. Engheta and R. W. Ziolkowski, *Metamaterials: Physics and Engineering Explorations* (Wiley-IEEE, New York, 2006)

[24] D. Schurig et al., *Science* **314**, 977–980 (2006)

[25] Y. Liu and X. Zhang, *Chem. Soc. Rev.* **40**, 2494–2507 (2011)

[26] L.-H. Wu and X. Hu, *Phys. Rev. Lett.* **114**, 223901 (2015)

[27] W.-J. Chen et al., *Nature Commun.* **5**, 5782 (2014)

[28] W.-J. Chen, Z.-Q Zhang, J.-W. Dong, and C. T. Chan, *Nat. Commun.* **6**, 8183 (2015)

[29] F. J. Garcia-Vidal, L. Martín-Moreno, and J. B. Pendry, *J. Opt. A: Pure Appl. Opt.* **7**, S97 (2005)

[30] S. Maci, G. Minatti, M. Casaletti, and M. Bosiljevac, *IEEE Antennas Wireless Propag. Lett.*, vol. **10**, 1499–1502, 2011.

[31] B. H. Fong, J. S. Colburn, J. J. Ottusch, J. L. Visher, and D. F. Sievenpiper, *IEEE Trans. Antenn. Propag.*, **58**(10), 3212–3221 (2010)

[32] H. J. Bilow, *IEEE Trans. Antenn. Propag.* **51**(10), 2788–2792 (2003)

[33] F. Elek, B. B. Tierney, and A. Grbic, *IEEE Trans. Antenn. Propag.* **63**(9), 3956–3962 (2015)

[34] R. Quarfoth and D. Sievenpiper, *IEEE Trans. Antenn. Propag.*, **63**(10), 4593–4599 (2015)

[35] A. M. Patel and A. Grbic, *IEEE Trans. Antenn. Propag.* **59**(6), 2087–2096 (2011)

[36] H. Wakatsuchi, S. Kim, J. J. Rushton, and D. F. Sievenpiper, *Phys. Rev. Lett.* **111**, 245501 (2013)

[37] P.-Y. Chen and A. Alù, *Phys. Rev. B* **84**, 205110 (2011)

[38] Z. Lou, X. Chen, J. Long, R. Quarfoth, and D. Sievenpiper, *Appl. Phys. Lett.* **106**, 211102 (2015)

[39] Ramo, Whinnery, Van Duzer, *Fields and Waves in Communication Electronics*, 2nd ed. (John Wiley and Sons, New York, 1984)

[40] D. F. Sievenpiper, *High-Impedance Electromagnetic Surfaces*. PhD thesis (UCLA, 1999)

[41] Jian-Ming Jin, *Theory and Computation of Electromagnetic Fields*, 1st ed. (Wiley, New Jersey, 2010)

[42] M. Lei, S. Xiao, J. Long, and D. F. Sievenpiper, *IEEE Trans. Antenn. Propag.* **64**(9), 3811–3819 (2016)

[43] A. Alu and N. Engheta, *IEEE. Trans. Antenn. Propag.* **51**(10), 2558–2571 (2003)

---

- [44] X. Shi, C. Xue, H. Jiang, and H. Chen, [Opt. Exp. 24\(16\), 18580 \(2016\)](#)
- [45] M. Xiao, Z. Q. Zhang, and C. T. Chan, [Phys. Rev. X 4, 021017 \(2014\)](#)
- [46] F. J. Lawrence, L. C. Botten, K. B. Dossou, R. C. McPhedran, and C. M. deSterke, [Phys. Rev. A 82, 053840 \(2010\)](#)
- [47] M. Xiao, X. Huang, A. Fang, and C. T. Chan, [Phys. Rev. B 93, 125118 \(2016\)](#)
- [48] X. Huang, Y. Yang, Z. H. Hang, Z.-Q. Zhang, and C. T. Chan, [Phys. Rev. B 93, 085415 \(2016\)](#)
- [49] J.-Y. Ou, J.-K. So, G. Adamo, A. Sulaev, L. Wang, and N. I. Zheludev, [Nat. Commun. 5, 5139 \(2014\)](#)
- [50] A. F. Koenderink, A. Alù, A. and Polman, [Science 348, 516–521 \(2015\)](#)
- [51] E. Forati, T. J. Dill, A. R. Tao, and D. Sievenpiper, [Nat. Commun. 7, 13399 \(2016\)](#)
- [52] X. Cheng et al., [Nature Mater. 15, 542–548 \(2016\)](#)
- [53] A. Vakil and N. Engheta, [Science 332, 1291–1294 \(2011\)](#)
- [54] M. Kauranen and A. V. Zayats, [Nature Photonics 6, 737–748 \(2012\)](#)